Behavior of unbonded multistrand posttensioning anchorage systems under monotonic and cyclical loads

Daniel A. Abramson, Eric S. Musselman, and Sri Sritharan

- This paper presents results from a comprehensive laboratory evaluation of the fracture and ultimate strength and strain capacities of multistrand posttensioning anchorage systems for use in seismic resilient rocking structures.
- The testing program encompassed two anchorage manufacturers, two anchorage alignment configurations, and two wedge geometries under both monotonic and cyclic loading.
- The results show that modifying the wedge geometry can improve the performance of commercially available posttensioning anchorages and that a strain limit of 1% should be used for seismic applications.

The growing popularity of unbonded posttensioned structural systems designed for seismic resiliency, in conjunction with recent research indicating the inability of posttensioning anchorage systems to meet current industry certification standards, has prompted the need to further test and better understand posttensioning anchorages. Posttensioning anchorage systems are required to develop a minimum elongation and percentage of the strand's capacity under tensile loads. ACI 423.7-14,[1] ACI 423.3-05,[2] and PTI M10.2-00[3] require anchorage systems to develop 2% elongation and 95% of the strand's measured tensile strength, while ACI 318-14[4] requires 2% elongation and 95% of the specified tensile strength. While strand manufacturers routinely meet these requirements, they use a special gripping device, which is 8 to 10 in. (200 to 250 mm) long. Commercially available wedge grips can be as small as 1.4 in. (36 mm) in length, which routinely cause the failure of the seven-wire strand in a posttensioning system at values below the standard requirements for the strands. Notching of the strand by the wedges and an unevenly distributed load over the length of the wedge at high stress levels cause stress concentration at the nose of the wedge and premature fracture of an individual wire.

Recent research has focused on single-strand posttensioning anchorages in an attempt to better understand the failure mechanisms and quantify the dependable ultimate strengths and strain capacities of these systems.[5–8] These studies found that failure of the strand in single-strand systems can occur at strains as low as 1%, well below the

current applicable limits. However, in structural systems, multistrand tendons are typically used; therefore, single-strand test results may not be applicable. Furthermore, no published literature is available in the United States regarding the performance of multistrand anchorages because the Post-Tensioning Institute (PTI) recommends testing only one strand at a time in multistrand anchorages.[9] It is possible that anchor manufacturers conduct anchorage validation tests, but the results of these tests are typically not publicly available. These uncertainties, as well as the necessity to better understand the unique phenomena that exist in multistrand systems loaded with multiple unbonded posttensioning strands at once, call for a comprehensive evaluation of multistrand posttensioning anchorage systems to establish suitable strain and stress limits that are appropriate for routine design.

Currently, there is considerable variation among governing institutions and code-writing bodies regarding the allowable reduction in strand capacity due to the observed premature failure when tested with standard wedge grips. This is largely due to recent changes in certification procedures promulgated by PTI and subsequently accepted by the American Association of State Highway and Transportation Officials (AASHTO) and the departments of transportation of many states.[10] In the mid-1990s, PTI replaced the term *guaranteed ultimate tensile strength* (GUTS) with two definitions: *minimum ultimate tensile strength* (MUTS) and *actual ultimate tensile strength* (AUTS).[11] GUTS is the tensile strength of the strand ensured by the manufacturer and is expressed as a stress (that is, force per area). AUTS is the actual breaking strength obtained in free-length fracture tests of a single representative strand and is expressed as a force. MUTS is the force equal to the nominal cross-sectional area of the strand times its nominal ultimate tensile strength.

Previously, PTI certification required anchorage systems to provide a minimum of 95% of GUTS. However, the new PTI certification requires the anchorages provide a minimum of 95% of AUTS, which can be significantly greater than GUTS. This change has made the certification requirement considerably more stringent by effectively increasing the required strength of the system. This is not because of the inadequate strength of the strands, but rather due to premature failure of the strands at the anchorage. Consequently, posttensioning anchoring devices commonly used in practice now fail certification testing in a substantial number of cases.[5,8]

However, not all code-writing bodies have accepted this new criterion, the most notable of which is the American Concrete Institute (ACI) in their *Building Code Requirements for Structural Concrete (ACI 318-14) and Commentary (ACI 381R-14)*.[4] Section 25.8.1 of ACI 318-14 requires that posttensioning anchorages develop at least 95% of the specified tensile strength of the prestressing steel f_{pu} and conform to the 2% elongation requirements in ACI 423.7[1] when tested in an unbonded condition, which is essentially the old PTI requirement. The 2% elongation requirement is to ensure sufficient ductility.

One application in which the performance of these anchorage systems is critical to the design is precast concrete structures designed for seismic resilience. Instead of the emulation concept that replicates the response of cast-in-place concrete structures, the precast concrete industry introduced the jointed concept to promote more favorable seismic response for precast concrete frames and wall buildings through the PRESSS (Precast Seismic Structural Systems) program.[12–14] A primary component of a jointed connection is multistrand unbonded posttensioning through the interface, which promotes a rocking mechanism for seismic-force-resisting members at their ends at the connection interface. This mode of response, as opposed to forming a plastic hinge, minimizes structural damage. The unbonded posttensioning also facilitates the self-centering capability of the precast concrete structural system and allows it to recenter when the lateral earthquake loads are removed. These unique features, which help to promote seismic resilience, have contributed to the growth of precast concrete seismic solutions (for example, Sritharan et al.[15]). Due to recognition of its unique benefits, unbonded posttensioning has now been applied to seismic-resistant structures designed with other construction materials, such as steel, masonry, and timber. For such structural systems to produce the expected seismic response, the design of the posttensioning tendons, including their anchorage, should be accomplished reliably. Consequently, the design documents developed for these systems enforce varying stress or strain limits for the unbonded posttensioning tendons, even though they are not supported by experimental data. For example, ACI Innovation Task Group 5 developed recommendations for the design of special concrete walls that aim to limit the stress in prestressing tendons at the design drift to below the yield strength of the posttensioning steel.[16] The investigation reported in this paper facilitates the definition of more reliable limits for use in design practice.

Research objectives

In recognition of the aforementioned knowledge gap, the primary objectives of this research are the following:

- to investigate the failure mechanisms as well as the ultimate strength and strain capacities of representative multistrand posttensioning anchorage configurations under monotonic and cyclic tensile loading
- to make recommendations for the acceptance testing of unbonded multistrand posttensioning anchorage systems

- to make recommendations for the design of unbonded multistrand posttensioning systems for use in seismic-resilient structures

Research program

To understand the behavior of strand anchorage, an experimental research program was planned and executed using both single-strand and multistrand posttensioning anchorage systems. The outcomes of the testing conducted on single strands are presented in Musselman et al.;[8] the details of the multistrand testing program are summarized in following sections.

Test setup

The test specimen consisted of multihead anchorages, strands, and wedge components oriented vertically in a 600 kip (2670 kN) material testing system load frame and pulled in tension to failure via upward displacement of the top fixture as regulated by the hydraulic cylinder. **Figure 1** is a schematic of the test setup with each element labeled.

A few additional components were necessary so that the laboratory test setup effectively replicated a field posttensioning system. Bearing plates were installed on the top and bottom material testing system fixtures to provide a uniform surface for the wedge plates (anchorages) to bear against. The bearing plates essentially replicated the bearing anchor in a field application. The bearing plates were designed to be compatible with anchorages from different manufacturers. In addition, the bearing plates allowed all strands to pass freely through a center hole in the bearing plate and the bottom of the test fixture while centering each wedge plate to ensure alignment between the top and bottom wedge plate.

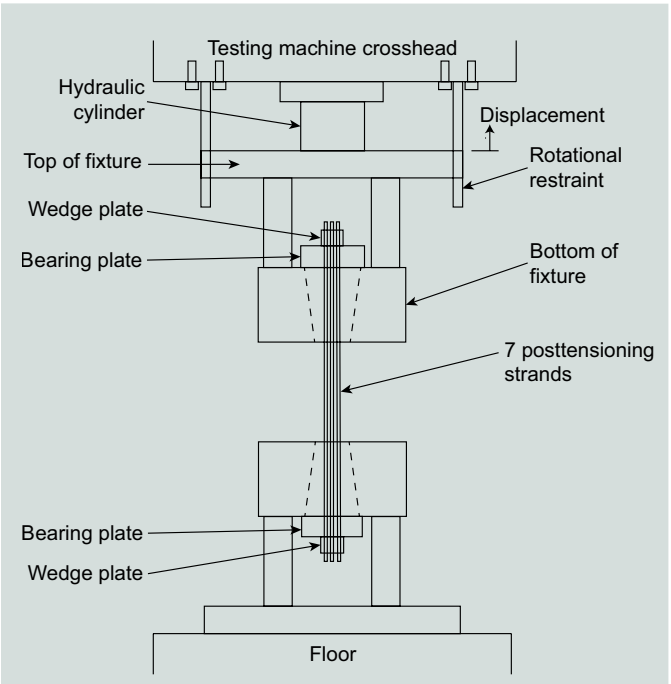

Figure 1. A schematic of the test setup.

A rotational restraint was installed on the top of the material testing system machine to prevent the top material testing system fixture from rotating during loading of the test specimen while allowing the fixture to move freely in the vertical direction. This restraint is provided in the field by friction between the posttensioning components and the torsional resistance of the structural element being posttensioned. The bottom material testing system fixture was incapable of rotating because it was fixed to the laboratory floor.

Test specimens

Each test specimen was made up of seven 7-wire posttensioning strands, two wedge plates, and fourteen wedges. **Figure 2** provides drawings of each component. **Table 1** lists the dimensions of each component taken as the average of the measured value at a minimum of three locations. The naming conventions used for component dimensions are consistent with previous research.[5]

All posttensioning strands came from a single spool of 0.6 in. (15 mm) diameter, Grade 270 (1860 MPa), low-relaxation, uncoated, seven-wire steel strand conforming to ASTM A416.[17] The strand had an actual breaking strength of 62.393 kip (277.52 kN), modulus of elasticity of 28,500 ksi (196.5 GPa), and cross-sectional area of 0.2227 in.^{2} (143.7 mm^2) as determined by the strand manufacturer and reported on the strand mill certificate of inspection. The strand was cut to approximately 50 in. (1270 mm) to ensure a final free length of at least 42 in. (1070 mm) from wedge nose to wedge nose. Actual strand free lengths varied from 42 to 45 in. (1140 mm) due to variability in seating of the wedges and overall anchorage height.

Anchorages from two manufacturers were evaluated. The anchorages are round with six tapered through holes positioned symmetrically around a center tapered through hole. The through holes are shaped to accept conical wedges that grip the strand. Both anchorages were of the same type: 0.6 in. (15 mm) seven-strand anchorages. Anchorages from manufacturer A were made of cast ductile iron conforming to ASTM A536.[18] Anchorages from manufacturer B were made of forged steel. Both anchorages are components of systems commonly used in the U.S. bridge and building industry. Anchorage alignment was evaluated during testing. For some of the tests, the anchors were aligned such that all strands were vertical, while in other tests, the anchors were intentionally rotated 135 degrees about the vertical axis, causing the strands to exit the anchorage at an

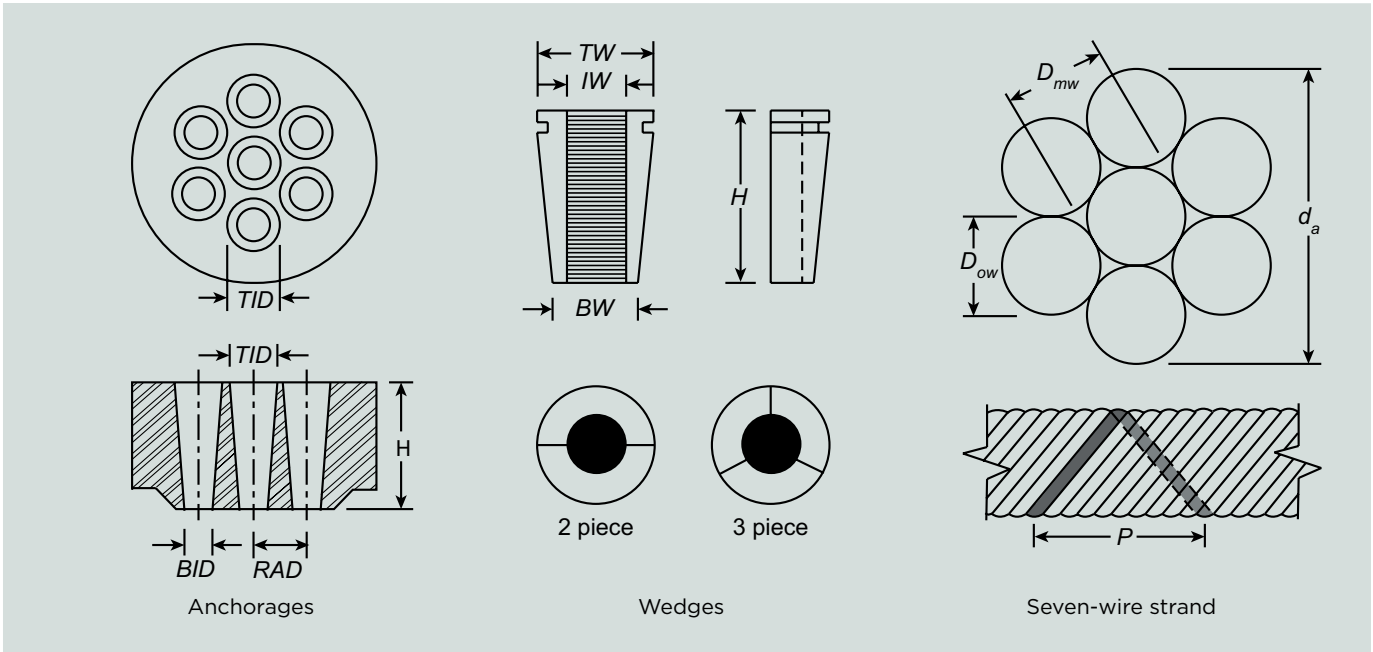

Figure 2. Test specimen components (not to scale). Note: *BID* = inside diameter of anchor bottom; *BW* = outside width of wedge bottom; d_a = outside crown-to-crown diameter of prestressing strand; D_{mw} = diameter of middle prestressing strand wire; D_{ow} = diameter of outer prestressing strand wire; *H* = height of component; *IW* = inside width of wedge; *P* = pitch of prestressing strand; *RAD* = distance from centerline of anchor to centerline of wedge opening; *TID* = inside diameter of anchor top; *TW* = outside width of wedge top.

angle. This modification was to represent possible twisting of strands when they are installed inside a long structural member.

Posttensioning wedges are typically formed by machining or forging a single truncated, cone-shaped metal body from a soft steel alloy. A hole is typically drilled in the cone-shaped metal body and the gripping elements are formed inside the hole via threading. Common threads used for testing include so-called *buttress* threads. The exterior surface of each wedge segment is smooth and tapered such that a small diameter exists on one end. The wedge segments are formed such that when applied to the exterior of the strand there is a gap between the circumferential ends

Table 1. Measured dimensions of specimen components

Anchorages		***H*, in.**	***TID*, in.**	***BID*, in.**	***RAD*, in.**
	Manufacturer A	2.76	1.15	0.70	1.31
	Manufacturer B	2.16	1.11	0.66	1.38
Wedges		***H*, in.**	***TW*, in.**	***BW*, in.**	***IW*, in.**
	2P-A standard	1.77	1.12	0.71	0.56
	3P-B standard	1.65	0.95	0.59	0.44
	2P-A balanced	1.77	1.12	0.70	0.57
	2P-B balanced	1.66	1.14	0.73	0.57
Seven-wire strand		**D_{mw}, in.**	**D_{ow}, in.**	**d_a, in.**	***P*, in.**
	0.6A	0.205	0.198	0.605	7.9625

Note: All dimensions are shown in Fig. 2. *BID* = inside diameter of anchor bottom; *BW* = outside width of wedge bottom; d_a = outside crown-to-crown diameter of prestressing strand; D_{mw} = diameter of middle prestressing strand wire; D_{ow} = diameter of outer prestressing strand wire; *H* = height of component; *IW* = inside width of wedge; *P* = pitch of prestressing strand; *RAD* = distance from centerline of anchor to centerline of wedge opening; *TID* = inside diameter of anchor top; *TW* = outside width of wedge top. 1 in. = 25.4 mm.

of each wedge segment. This enables lateral compression against the strand as the wedge is moved into the receiving bore. Wedges are often heat treated to obtain a surface hardness of about 58 to 64 Rockwell C so that the gripping element of the wedge (threads) can deform the exterior surface of the strand.[10]

Four different wedge geometries were tested, all produced (but not necessarily designed) by the same manufacturer. Two-piece wedges are differentiated from three-piece wedges by the naming convention of 2P and 3P, respectively. The wedge geometries were as follows:

- 2P-A standard: two-piece wedges for the anchorage designed by manufacturer A (anchorage A)
- 3P-B standard: three-piece wedges for the anchorage designed by manufacturer B (anchorage B)
- 2P-A modified: two-piece wedges for anchorage A, designed by the wedge manufacturer to more evenly balance the stresses within the wedge during peak loading
- 2P-B modified: two-piece wedges for anchorage B, designed by the wedge manufacturer to more evenly balance the stresses within the wedge during peak loading

The performance of the two-piece wedges was not compared directly with the performance of the three-piece wedges in this study. Rather, the number of wedge pieces was simply determined by whoever provided the wedges. For the wedges denoted by *standard*, the anchorage manufacturer provided wedges just as they would to a contractor in a field application (that is, the wedge type was not specified when ordering the anchorages). Thus, the shift from two-piece to three-piece standard wedges from manufacturer A to manufacturer B was simply the product of differences in the wedge geometry preferred and designed by each respective manufacturer. For the wedges denoted by *modified*, the wedge manufacturer designed the wedges based on the dimensions of each anchorage. This manufacturer always designs its modified wedges as two-piece wedges because of the additional quality control complications introduced with producing three-piece wedges.

The physical change in wedge geometry that allows a more balanced load along the gripped length of strand is the product of two primary principles: angle differential and gap control. The principle of angle differential relates to the taper angle of both the anchor and wedge. The standard wedges have a geometry in which the taper angle of the exterior surface of the wedge matches the seven-degree taper angle of the wedge receiving bore.[19] This type of wedge geometry, which is the current industry standard, forces all of the wedge teeth to engage on the strand simultaneously when loading begins. Once the entire wedge length has engaged, elongation of the strand within the anchorage is significantly restrained. Thus, the load along the length of the wedge is concentrated at the nose. This so-called *elongation nose loading* begins early in the loading and propagates as loading continues. Eventually, this stress concentration causes the shear failure of an individual wire within the anchorage at the nose of the wedge.

Alternatively, the modified wedges have an exterior surface taper angle that is one to two degrees greater than that of the wedge-receiving bore. This difference in angle allows the wedge to grip the strand sequentially from the back, or wide end, of the wedge to the nose, or narrow end of the wedge, as the load increases. This fundamental change in the engagement of wedge teeth allows elongation of the strand to occur within the wedge throughout loading and up to failure. As a result, the normal force on the strand along the length of the wedge is more balanced as the load approaches the actual free-length breaking strength of the strand.

The second principle of the modified wedge geometry is gap control.[10] When wedges are placed around the strand prior to loading, an initial (uncompressed) gap exists between adjacent wedge pieces along the longitudinal axis of the strand. As the prestressing force increases, the wedge pieces compress laterally, closing this initial gap. If the gap between wedge pieces is allowed to close completely, the wedges are no longer able to move inward and grip the strand as the load increases. This leaves the system potentially susceptible to a pull-out failure in which the gripping force of the wedge is no longer sufficient to restrain the tensile force of the strand.

The standard wedges have a geometry such that the wedge pieces remain in free float (that is, will never come in contact) throughout the loading sequence.

Alternatively, the wedge manufacturer has determined experimentally that allowing the wedge pieces to come into contact, with reasonable limitation, is actually beneficial to the operation of the anchor system overall.[10] The modified wedges are manufactured to have a smaller, uncompressed gap between the wedge pieces. When this smaller initial gap is implemented, the centering movement of the wedges is stopped late in the loading sequence due to the wedge pieces coming into contact. This allows the wedges to penetrate the exterior strand wires just enough to avoid a pull-out failure without overpenetrating the strand.

Instrumentation

The data acquisition system provided elapsed time in seconds, total load in kips, crosshead displacement in inches, and strain gauge readings in microstrain. The load data from the internal material testing system load cell was important

for determining the stress within the system. However, the load reading was a total for the entire system (that is, the load on each individual strand was not recorded). Due to the ductile nature of the strand and the continuation of loading beyond its yielding, the strain data is generally more meaningful than the load data from an analysis standpoint. In addition, the individual strain of each strand was recorded, which allowed for a better understanding of how load is distributed through the system. For that reason, more emphasis is placed on strain data instrumentation and analysis.

The strain instrumentation required by the International Code Council Evaluation Service's (ICC-ES's) *Acceptance Criteria for Post-Tensioning Anchorages and Couplers of Prestressed Concrete* is a 36 in. (910 mm) extensometer.[20] However, previous research has demonstrated that in the case of unbonded posttensioning strands, extensometer gauge length does not appreciably affect the strain measurements.[5] In addition, strain gauges have been investigated as an instrumentation system for posttensioning strands in a laboratory setting, testing strand directly, and in segmental box girder bridges, with positive results.[8,21,22] Therefore, the primary method of collecting strain data in this study was with electrical resistance strain gauges fixed to an individual wire of each of the seven strands (that is, seven strain gauges per strand).

The strain gauges used had a gauge length of 0.04 or 0.08 in. (1 or 2 mm) as availability of strain gauges of this size was limited. Strain gauge locations varied depending on whether both anchorages were aligned so that the strands were vertically parallel or one anchor head was rotated causing the strands to touch at the midheight of the specimen. When the anchorages were aligned, the strain gauges were located at the midheight of the specimen. Although the assumption has already been stated that the local strain along the length of the strand is constant, strain gauges were placed at midheight for consistency and to avoid damaging the strain gauges during installation and seating of the strands. When one anchorage was rotated, the strain gauges were located 9.5 in. (240 mm) above the midheight of the specimen. This was done to avoid damaging the strain gauges when the strands rubbed against each other during rotation. **Figure 3** shows the vertical location of the strain gauges on the strands.

Optical position tracking was implemented as an alternative method of measuring strain. The position sensor uses high-speed, real-time digital photogrammetry and optical triangulation techniques to track the precise three-dimensional position of markers. Strain can then be calculated based on the change in distance between the markers divided by the initial distance between them. This alternative method of strain measurement was implemented for a selected number of trials to verify the strain data collected by strain gauges and to test the usefulness of optical strain

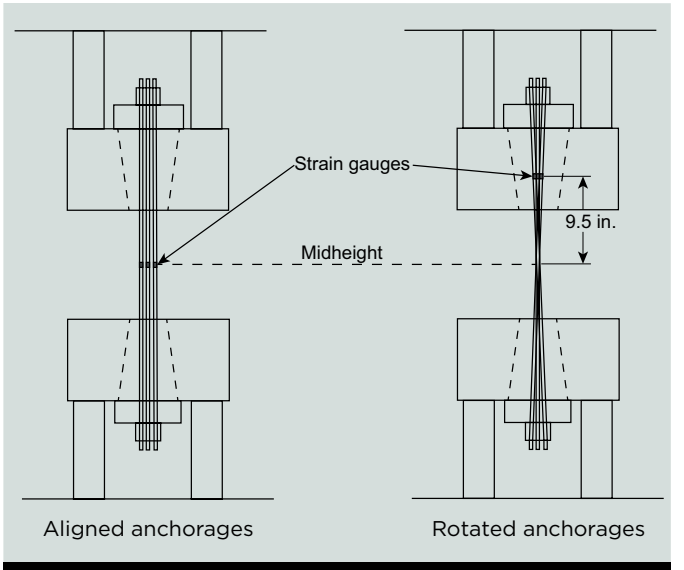

Figure 3. Elevation view of strain gauge locations. Note: 1 in. = 25.4 mm.

measurement on posttensioning strands. The optical strain measurements did not replace those of the strain gauges for these selected trials; rather, the two methods were used simultaneously to verify the data. The data from the optical strain measurements also helped to compare strand strain with individual wire strain to verify the analytical approximation developed by Acosta relating wire strain to strand strain based on the wire pitch and strand diameter.[22]

Four markers spaced at 2 in. (50 mm) were fixed on three or four strands per test for rotated or aligned anchorages, respectively. The markers were placed around the strain gauges so that the local strain in that region could be effectively compared. The optical strain measurements were based on the elongation of the strand because the markers were too large to mount to the individual wires, in contrast with the strain gauges, which recorded the elongation of the individual wires. The markers were typically affixed to two or three wires. **Figure 4** shows several markers mounted to four strands and the top and bottom material testing system fixtures for an aligned anchorage test.

Sample preparation

The first step was to prepare the strands by attaching the strain gauges. This was done prior to installing the strands in the material testing system frame to allow ample time for the strain gauge adhesive to cure without delaying testing. The seven strands were placed in the testing frame by feeding them vertically through the top anchorage and applying light pressure to one wedge per strand, leaving approximately 1.25 in. (31.8 mm) of strand overhang. The material testing system crosshead was then raised and each strand was fed through the bottom anchorage, ensuring proper alignment of each strand with the top anchorage.

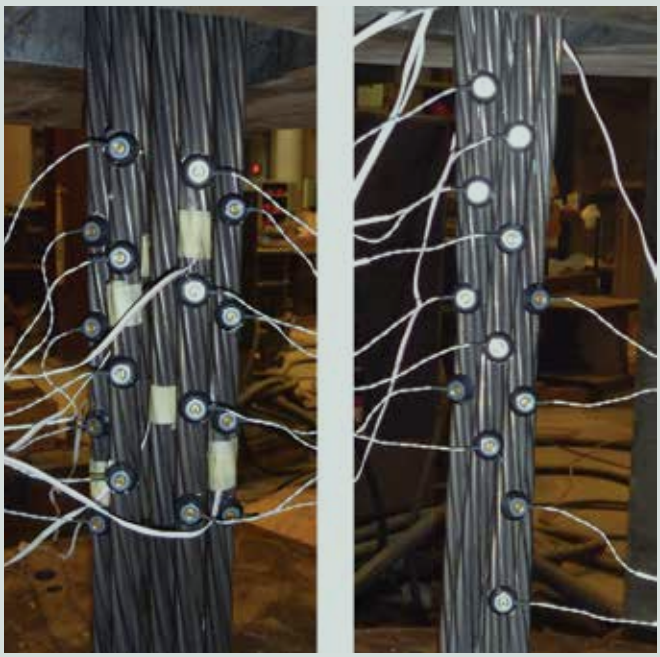

Aligned anchorages Rotated anchorages

Figure 4. Optical tracking markers fixed to strands and testing fixtures.

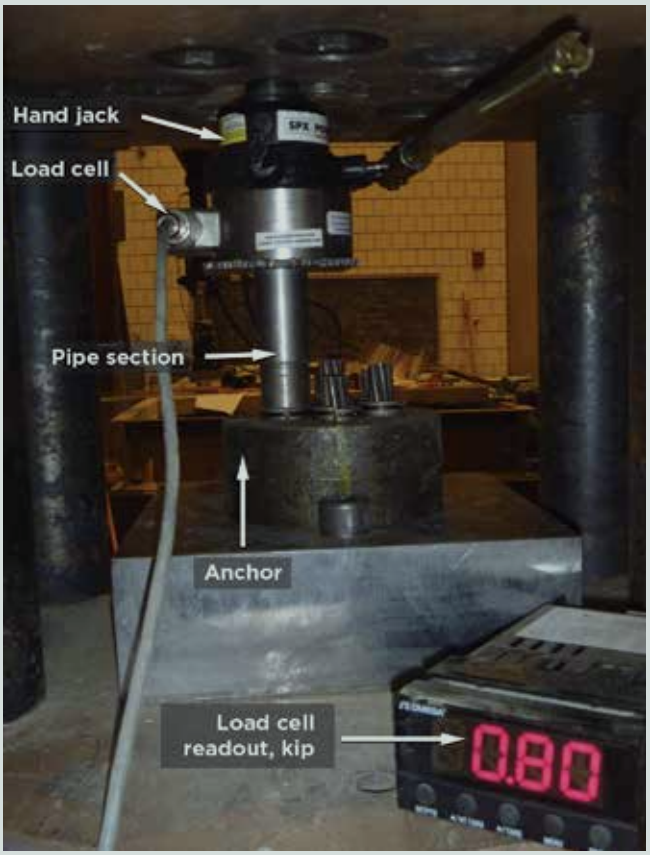

Figure 5. Initial seating apparatus. Note: 1 kip = 4.448 kN.

Again, light pressure was applied to one wedge per strand to hold that bottom anchor in place, with at least 1.25 in. of the strand extending beyond the ends of the wedges. However, for the bottom wedges, greater emphasis was placed on ensuring that each wedge was at the same elevation in order to ensure even loading of each strand during testing. If the test configuration called for a rotated anchor head, rotation of the bottom anchorage took place at this time.

Next, an initial seating was completed by applying a force of 800 lb (3560 N) directly to the top and bottom wedges using a low-profile hydraulic hand jack, a small load cell, and a pipe section (**Fig. 5**). A force of 800 lb was chosen based on the ICC-ES report AC303 requirement that the applied preload (seating load) not exceed 1000 lb (4450 N) for a monostrand system.[20] The seating procedure was implemented to ensure consistent wedge seating depths and forces with the goal of loading each of the seven strands as evenly as possible. This initial seating procedure emulates the dead-end seating procedure in field applications where the wedges are initially seated by hand with additional seating occurring as the strand is stressed from the other end.

Strain gauge lead wires were then attached to the strain bridge, and markers were attached to visible strands, if applicable. A preload between 5 and 7 kip (22 and 31 kN) was then applied to the seven-strand anchorage to further seat the wedges and take up any remaining slack in the system. This level of preload was again based on the ICC-ES AC303 requirement that the preload per strand should not exceed 1000 lb (4450 N). The initial specimen length was measured, the anchorage ends protected to prevent flying objects, and offsets taken for strain and displacement. The specimen was then ready to be loaded.

Testing procedure

Monotonic and cyclic loading protocols were used in this study. Monotonic tests were conducted to set a baseline for multistrand anchorage performance. Cyclic tests were conducted to study the behavior of the posttensioning system under high-strain amplitude and low-cycle loads that can simulate the effects of seismic loads on the anchorage of unbonded tendons. The cyclic loading protocol was intended to replicate the effects of seismic loads on the anchorage of unbonded posttensioning tendons in rocking structural members, though the loading frequency was considerably slower than desired due to limitations of the testing equipment. The testing equipment allowed a frequency of 0.1 Hz, while testing conducted in another phase of this research program evaluated the behavior of rocking precast concrete walls and found that the corresponding prototype wall has a dominant response at a frequency of 0.35 Hz. Depending on the aspect ratio of the rocking structural member, the dominant frequency can vary significantly when subjected to a seismic input motion. The wall tests

further confirmed that the strain rate in the unbonded tendon varies at the same frequency as the rocking member.[23]

The monotonic and cyclic loading protocols were developed based on the ICC-ES document.[20] The testing procedures and requirements presented in ICC-ES AC303 are specifically for monostrand assemblages. Because no such document exists for the testing of multistrand assemblages in the United States, the monostrand guidelines in the ICC-ES document were applied as closely as possible to the multistrand tests discussed in this paper.

The monotonic loading protocol consisted of a constant, displacement-controlled load rate of 0.361 in. (9.17 mm) per minute, which corresponds to a strain rate of 0.0086 per minute for a 42 in. (1070 mm) long test specimen. This falls within the ICC-ES required strain rate of 0.0047 to 0.021 per minute. The loading occurred via upward displacement of the top fixture as regulated by the hydraulic cylinder, while the bottom anchor remained stationary.

The cyclic loading protocol consisted of three parts:

- ramp to lower bound of cyclical loading
- sinusoidal cyclic loading
- ramp to failure

The ramp to the lower bound of the cyclical loading step was intended to replicate the monotonic load rate of 0.361 in. (9.17 mm) per minute for stresses from zero to $0.20f_{pu}$. However, due to limitations of the testing software, this loading step was force controlled rather than displacement controlled. This led to crosshead displacement rates as high as 8.0 in. (200 mm) per minute for portions of the loading step while the wedges were seating. Although the desired crosshead displacement rate was exceeded, the strands were still loaded in a slow, controlled manner. In addition, the loading was within the ICC-ES guidelines because no maximum rate is specified for this step and 8.0 in. per minute is slower than the load rate implemented during the cyclic loading step.

The specimen was then cycled 50 times from $0.20f_{pu}$ to $0.85f_{pu}$ at 0.1 Hz. Several deviations from the ICC-ES document were required for this loading step due to limitations of the testing equipment and the anchorage capacities. The ICC-ES document calls for a cyclic frequency between 1 and 3 Hz and a cyclic stress range between $0.40f_{pu}$ and $0.85f_{pu}$. However, previous monostrand test results showed that a cyclic range of $0.40f_{pu}$ to $0.85f_{pu}$ was not large enough to cause any significant reduction in capacity of the system.[6] Thus, the lower limit of the cyclic range was reduced to $0.20f_{pu}$. Monostrand test results also indicated that an upper cyclic range of $0.85f_{pu}$ was not high enough to affect the system's performance or observe the type of postyield behavior desired.[6] However, because the monotonic multistrand tests conducted as part of the current study showed ultimate capacities as low as $0.88f_{pu}$, maintaining the ICC-ES recommended upper limit was considered appropriate. Finally, a cyclic frequency of 0.1 Hz was the maximum that could be achieved by the material testing system frame under such a large load range. Upon completion of 50 cycles, the specimen was pulled to failure at a constant displacement-controlled load rate of 0.361 in. (9.17 mm) per minute, which is consistent with the static tests.

Test matrix

Thirty-six specimens were tested in twelve unique configurations. As discussed, the four variables investigated were the following:

- loading protocol
- anchorage manufacturer
- anchorage alignment
- wedge geometry

Table 2 contains a summary of the testing configurations.

Data analysis

Two parameters were extracted and examined from the data taken during each test: stress within the strand and strain within the strand. The stress within the strands was derived from material testing system load cell data. The data acquisition system provided the total load, in kips, of the system. The load was then divided by the nominal cross-sectional area of the 0.6 in. (15 mm) seven-strand system (that is, 0.217 in.^{2} × 7 = 1.519 in.^{2} [980.0 mm^2]). This assumes that the load is uniformly distributed across each of the seven strands, which may introduce some uncertainty into the stress results.

Occasionally, an individual wire of a strand fractured at a stress level lower than the ultimate strength achieved by the system (**Fig. 6**). Therefore, two stress values are reported: fracture strength and ultimate strength. The fracture strength is the stress of the specimen at the time of initial wire fracture. The ultimate strength is the maximum stress that the specimen achieved. Consequently, the fracture strength may be equivalent to the ultimate strength if the initial fracture stress is the maximum stress that the specimen achieved, or the ultimate strength may exceed the fracture strength if the system achieved a higher stress level after initial fracture.

Table 2. Testing configurations summary

Loading scheme	Manufacturer	Alignment	Wedge type	Repetitions
Monotonic	A	Aligned	2P-A standard	3
		Rotated		3
	A	Aligned	2P-A balanced	3
		Rotated		3
	B	Aligned	3P-B standard	3
			3P-B standard	3
Cyclic	A	Aligned	2P-A standard	3
		Rotated		3
	A	Aligned	2P-A balanced	3
		Rotated		3
	B	Aligned	3P-B standard	3
			3P-B balanced	3
Total multistrand tests conducted				36

The strain gauge data was verified with the use of optical tracking equipment on a selected number of tests. Recording the strain of each strand was especially useful in understanding how the stresses were distributed throughout the system (that is, to each strand). As noted, the strain gauge data represented the strain in an individual wire rather than the actual elongation of the strand as a whole. For the purposes of making design recommendations for rocking structures, the strand elongation, and thus the system elongation, is the desired value. Unfortunately, it is difficult to use crosshead displacement data to calculate the system elongation because of wedge seating that occurs throughout much of the loading cycle—an effect that is magnified in a laboratory specimen with a relatively short free length. Thus, strain gauge data from an individual wire of each strand was considered to be representative of the system as a whole. This is a conservative assumption because the measured strain of an individual wire is approximately 3.8% to 6.8% lower than the strand at the same stress level.[20]

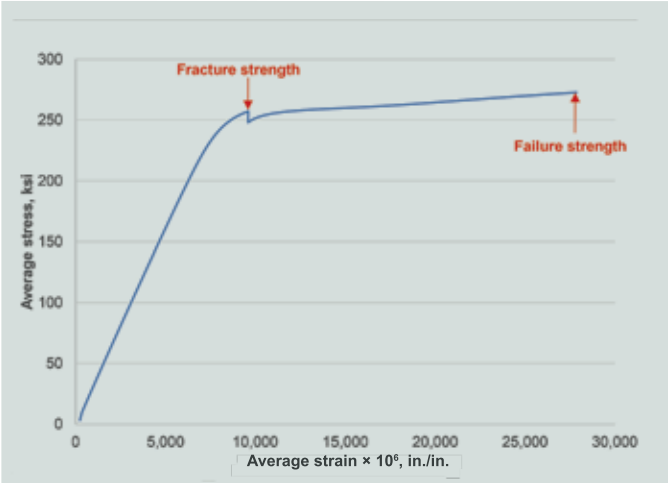

Figure 6. Stress-strain curve showing difference between fracture and ultimate stress for a seven-strand test. Note: 1 in. = 25.4 mm; 1 ksi = 6.895 MPa.

To remove any seating and differential offset effects, the strain gauge data was adjusted so that the linear portion ($0.20f_{pu}$ to $0.50f_{pu}$) of the stress-strain curve intersected the origin. Among the seven strands instrumented in each test, variability existed between the strain in each strand at a given load level. It is reasonable to assume that the variability in strain among the strands was greater in the test specimen than what would be observed in a full-scale system due to the relatively short length of strand being tested (that is, 42 in. [1070 mm] free-length minimum). The primary basis for justification of this assumption is the ratio of wedge seating depth to the total specimen length. In a 42 in. specimen, this ratio is approximately 0.95%, assuming a total wedge seating of 0.40 in. (10 mm) (0.20 in. [5 mm] at each end).[8] In a full-scale system (for example, 432 in. [10,970 mm]), this ratio would be approximately 0.093%. Therefore, the effects of slightly different levels of strand seating and wedge engagement would be negligible and the strains in each strand would be much closer together.

The aforementioned discrepancy in strain variability between the test specimen and a full-scale assemblage led to the strain being derived in terms of both the average and

maximum strain at fracture and ultimate (**Fig. 7**). Following are the resulting four types of strain derived from the strain gauge readings:

- average fracture strain: the average strain reading of all working strain gauges at the time of initial wire fracture
- maximum fracture strain: the maximum strain reading of all working strain gauges at the time of initial wire fracture
- average ultimate strain: the average strain reading of all working strain gauges at the time that the ultimate strength is achieved
- maximum ultimate strain: the maximum strain reading of all working strain gauges at the time that the ultimate strength is achieved

Because the definitions are based on working strain gauges, the reliability of the strain gages is important. For the majority of samples, all seven gauges functioned throughout the duration of the test. The average strain, which is calculated as a straight average of all working strain gauges at a particular time, is the more conservative strain measurement. In this calculation, it is assumed that if one strand is loaded early, the other six strands would experience a reduced strain at a given load. Thus, an average of all seven strains provides the actual system strain. Although this approach makes sense conceptually, it is likely overly conservative. The maximum strain is simply taken as the maximum value of all working strain gauges at a particular time. In the test specimen, the strand with the greatest strain represents the true maximum strain that an individual strand in the system can withstand. Considering this fact, it is reasonable to assume that the maximum strain measured in the 42 in. (1070 mm) test specimen is the most representative value of the limiting strain expected in a full-scale system where the strain in each strand is more consistent.

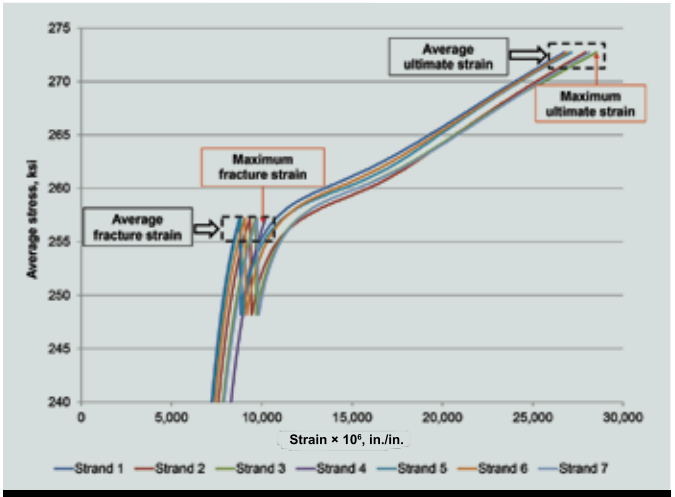

Figure 7. Average and maximum fracture and ultimate strain definitions using data from a seven-strand test. Note: 1 in. = 25.4 mm; 1 ksi = 6.895 MPa.

The optical position tracking data acquisition system was independent from the material testing system. For this reason, the two data sets were aligned based on the crosshead displacement. The strain in a strand from the optical position data was derived by calculating the change in three-dimensional Euclidean distance between two markers on a strand and dividing by their initial distance. It was determined that the derived strain, calculated using an average of three distances between all four markers spaced at 2 in. (50 mm) each, was equivalent to the derived strain calculated using simply the uppermost and lowermost markers spaced at 6 in. (150 mm). Thus, the derived strain was calculated considering only the uppermost and lowermost markers on a strand.

At low stress levels, the strands tended to twist and straighten while initial seating and engagement of each wedge occurred, and any remaining slack in the system was removed. If this out-of-plane motion is not properly accounted for, it will be interpreted as strain using the derived strain equation. In addition, this portion of the curve cannot simply be eliminated or zeroed because some amount of strand elongation occurs during this time. Therefore, a graphical method was implemented to determine the initial distance between markers. First, the distance between the uppermost and lowermost markers was plotted against load. A best-fit line was then applied over the portion of data corresponding to a linear range from $0.20f_{pu}$ to $0.50f_{pu}$ using the least squares method. The intersection of the best-fit line with the distance axis was then taken as the initial distance when calculating the strain in the strand.

Experimental results

The results of the multistrand anchorage tests are presented in terms of both strengths and strain capacities, and these results are compared with the current design limits. However, discrepancies arise in the terminology of certification requirements because they are currently intended for strand/anchorage systems in which only a single strand is being tested. In terms of strength requirements, ICC-ES AC303 states, "Each test assembly shall demonstrate failure of the strand at a test load of at least 95% of the actual breaking strength of the strand used in the tests."[20] For a multistrand test assembly, the failure load is interpreted as the load at the first wire fracture. However, the ICC-ES deformation requirement states, "The elongation of the strand of each tested assembly at the ultimate load shall be at least 2 percent."[20] As discussed previously, for a multistrand test assembly, the ultimate load may not correspond to the fracture load. Due to this difference in terminology, for the purpose of determining certification conformance, the

fracture stress of the system is compared with the stated strength limit, while the ultimate strain of the system is compared with the stated deformation limit.

The 2% elongation noted previously is routinely achieved by the strand manufacturers using special wedges, which rely on sand to provide friction instead of the teeth on a typical wedge and transfer the load to the strand over a longer length, both of which help to reduce stress concentrations. However, this elongation may not be applicable for designing rocking, self-centering structures, in which case regular commercially available wedges are used. Furthermore, fracture strain is of the utmost importance to the design engineer because an individual wire fracture during a seismic event will likely require replacement of the posttensioning. Thus, for the purpose of making design recommendations, the fracture strain is cited as the limiting condition, though all critical strains are reported.

Strain gauge verification

Two different criteria were used to compare the data obtained from the strain gauges with the data obtained from the optical position system: the calculated modulus of elasticity and failure strain of the system. The modulus of elasticity was determined using the method described by Acosta.[22] In this procedure, a best-fit line of strain in each strand (using either strain gauge or optical position data) was computed considering only the data points that corresponded to stresses between $0.20f_{pu}$ and $0.80f_{pu}$. The combination of modulus of elasticity and failure strain allows for the optical position and strain gauge data to be compared over both the elastic and inelastic ranges. **Table 3** shows the results of that comparison as a ratio of the strain gauge data to optical position data. The data show that the strain gauges consistently measure less strain than the optical position system. This is consistent with the results reported by Acosta,[22] who estimated this ratio to be between 0.936 and 0.963 depending on the pitch of the individual wires within the strand. The data obtained in this study shows a lower ratio of about 0.91, which is outside of the expected range. While these findings support the fact that the strain gauges provided satisfactory and conservative data, a more robust study of the ratio between posttensioning strand and individual wire strain is required before strain gauge readings can be confidently converted to strand strain using this ratio.

Stress capacity

The strength of the multistrand posttensioning anchorage system was analyzed in terms of average engineering stress (that is, total load divided by the nominal cross-sectional area of all seven strands). **Figures 8** and **9** provide a summary of the stress capacity of the system under each configuration. Figure 8 shows the results for the monotonically loaded tests, whereas Fig. 9 shows the results from the cyclically loaded tests. Three repetitions were conducted for each configuration, which is represented by a vertical bar. The lower (solid) part of the bar represents the fracture strength of the system, and the upper (crosshatched) part of the bar represents the ultimate strength of the system. If the bar is completely solid, the ultimate strength is equal to the fracture strength.

Table 3. Measured dimensions of specimen components

	Ratio of strain gauge to optical position data		Theoretical ratio*
	Modulus of elasticity	Failure strain	
Maximum	0.964	0.949	0.963
Average	0.916	0.910	n/a
Minimum	0.881	0.867	0.936

Note: n/a = not applicable.
* Data from Acosta (1991).

Two stress limits suggested by design standards are also drawn on each graph. The lower line is the ACI 318-14 limit of $0.95f_{pu}$ (256.5 ksi [1769 MPa]). The upper line is the ICC-ES (and all others) limit of $0.95f_{pm,free\text{-}length}$ (273.1 ksi [1883 MPa]). The maximum free-length fracture strength $f_{pm,free\text{-}length}$ was taken as the breaking strength of the strand as reported by the manufacturer, which was presumably determined using special wedges, divided by the nominal cross-sectional area of the strand.

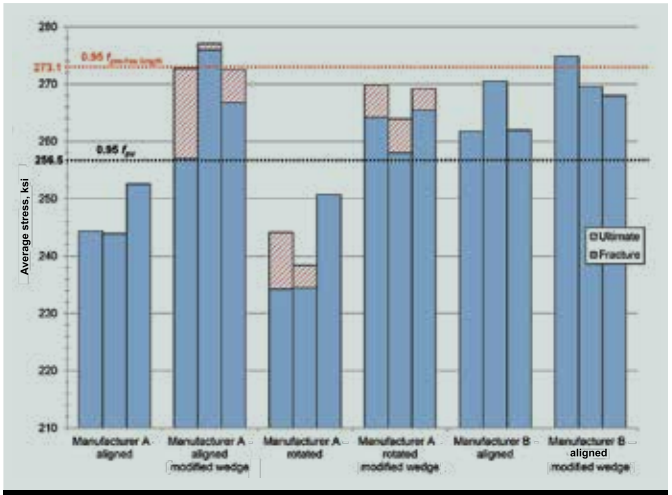

Figure 8. Summary of average stress results for monotonically loaded specimens. Note: $f_{pm,free\text{-}length}$ = free-length fracture stress calculated by dividing the breaking strength provided from a free-length fracture test by the nominal cross-sectional area of the strand; f_{pu} = specified ultimate tensile strength of prestressing strand. Note: 1 ksi = 6.895 MPa.

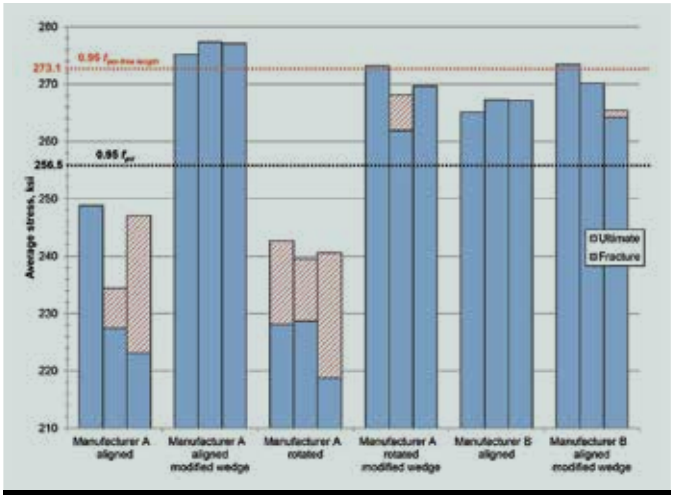

Figure 9. Summary of average stress results for cyclically loaded specimens. Note: $f_{pm,free\text{-}length}$ = free-length fracture stress calculated by dividing the breaking strength provided from a free-length fracture test by the nominal cross-sectional area of the strand; f_{pu} = specified ultimate tensile strength of prestressing strand. Note: 1 ksi = 6.895 MPa.

As shown in Fig. 8, anchorages from manufacturer A tested with standard wedges did not meet the ACI 318-14[4] strength requirement of $0.95f_{pu}$ at fracture. All of the other configurations, however, exceeded $0.95f_{pu}$ at fracture. On average, manufacturer A tested with aligned anchorage heads and modified wedges was able to reach $0.95f_{pm,free\text{-}length}$ at ultimate. However, the fracture strength, not the ultimate strength, is the limiting value for strength certification. Therefore, on average, none of the configurations met the $0.95f_{pm,free\text{-}length}$ limit when loaded monotonically.

The cyclically loaded specimens (Fig. 9) showed similar results to those loaded monotonically. Again, anchorages from manufacturer A tested with standard wedges did not meet the $0.95f_{pu}$ limit at fracture, while all other configurations did. The only change in performance occurred with manufacturer A with aligned anchorage heads and modified wedges. When subjected to the cyclic loading scheme, the specimen exceeded $0.95f_{pm,free\text{-}length}$ at fracture for all three repetitions.

Visual inspection of the bar graphs suggests qualitatively that the modified wedge geometry improves the performance of anchorages from both manufacturers and that anchorage rotation may reduce the strength capacity of the system. To quantify these apparent trends, a statistical analysis of fracture strength was conducted for each of the four test variables. By comparing tests in which only one variable changed, several direct comparisons could be drawn and statistically analyzed to determine whether a certain parameter caused a statistically significant change in the mean fracture strength capacity of the system.

Two-tailed Student's *t*-tests were used to evaluate the loading scheme, anchorage manufacturer, anchorage alignment, and wedge geometry variables. Student's *t*-tests are used to determine the probability of two data sets being statistically different from each other. The value that results from a *t*-test is called a *p*-value, and the meaning of this *p*-value depends on the type of *t*-test being run. When a two-tailed Student's *t*-test is used, the null hypothesis is that the two data sets have equivalent means. Therefore a low *p*-value indicates a small probability that the null hypothesis (data sets have equivalent means) is correct, and that there is a high probability that the data sets are statistically different. For all of the tests, it was assumed that the two populations are unpaired and have about the same spread (that is, they are homoscedastic). A method of variable elimination was implemented to increase the sample size of the tests being directly compared. For example, by showing statistically that no significant difference in means exists among monotonic and cyclic load tests, the loading parameter could be eliminated. Thus, when comparing manufacturer A with standard wedges to manufacturer B with standard wedges, fracture strengths from both monotonic and cyclic load tests were used. In addition, for this example, the anchorage alignment variable was eliminated because no rotated anchorage tests were conducted for manufacturer B.

Table 4 shows a summary of the results from the statistical analysis conducted for fracture strength. A 95% confidence interval was used to determine the significance of a selected variable. Thus, a *p*-value of less than 0.05 indicates a significant difference in means. This is displayed directly in the fourth column of Table 4 as an equal sign for variables with a *p*-value greater than 0.05 (not statistically different) and a less-than or greater-than sign as appropriate for variables with a significant difference in means.

For the loading scheme parameter, individual *t*-tests were conducted for each of the direct comparisons drawn in Table 4. The *t*-tests showed that none of these comparisons had a significant difference in their means. Thus, for the remainder of the statistical tests, the loading scheme parameter was eliminated as a unique variable (that is, tests that varied only by loading scheme were considered to be part of the same population).

For the statistical analysis of the anchorage manufacturers, the anchorage alignment variable was eliminated because alignment was not investigated for manufacturer B (that is, only the aligned anchorage tests for manufacturer A were compared with the aligned anchorage tests for manufacturer B). Therefore, the only variables remaining to compare were anchorage manufacturer and wedge geometry.

Figure 10 shows the box-and-whisker plot for manufacturers A and B when the standard wedges and modified wedge configuration were used. On this plot, the upper and lower whiskers indicate the maximum and minimum observed values, respectively. The bottom of the shaded box is the

Table 4. Fracture stress statistical analysis results summary

Variable	Configuration	Variable A	Equivalency	Variable B	*p*-value
Loading scheme	All	Monotonic	=	Cyclic	> 0.05
Anchorage manufacturer	Standard wedge	A	<	B	4.967×10^{-4}
	Modified wedge	A	=	B	0.6890
Anchorage alignment	Standard wedge	Aligned	=	Rotated	0.2765
	Modified wedge	Aligned	=	Rotated	0.1563
Wedge geometry	Manufacturer A aligned	Standard	<	Modified	3.249×10^{-4}
	Manufacturer A rotated	Standard	<	Modified	4.945×10^{-5}
	Manufacturer B aligned	Standard	=	Modified	0.0604

first quartile, the top of the crosshatched box is the third quartile, and where the boxes meet is the median value. The "X" on the plots indicates the mean of the data set. These plots demonstrate the difference in the mean and the spread of the data sets.

The calculated *p*-values for the standard and modified wedge configurations were 4.967×10^{-4} and 0.6890, respectively. This indicates that when each manufacturer uses its respective standard wedges, manufacturer B has a significantly greater mean fracture strength than manufacturer A. However, when the modified wedge geometry is used, the mean fracture strength of manufacturer A actually exceeds that of manufacturer B, but not to a statistically significant extent. The difference in anchorage performance among changing wedge geometries indicates that anchorage performance is highly dependent on anchor and wedge compatibility. That is, anchorage A is capable of performing as well as anchorage B when compatible wedge geometries are used.

Anchorage alignment was only investigated for anchorages from manufacturer A; therefore, the anchorage manufacturer together with the loading scheme parameter were eliminated for the investigation of the anchorage alignment. The only variables remaining to compare were anchorage alignment and wedge geometry. **Figure 11** shows the box-and-whisker plot for the aligned and rotated anchorages when the standard wedges and modified wedge geometries were used. The calculated *p*-values for the standard wedge and modified wedge configurations are 0.2765 and 0.1563, respectively. This indicates that while the mean fracture stress of the sys-

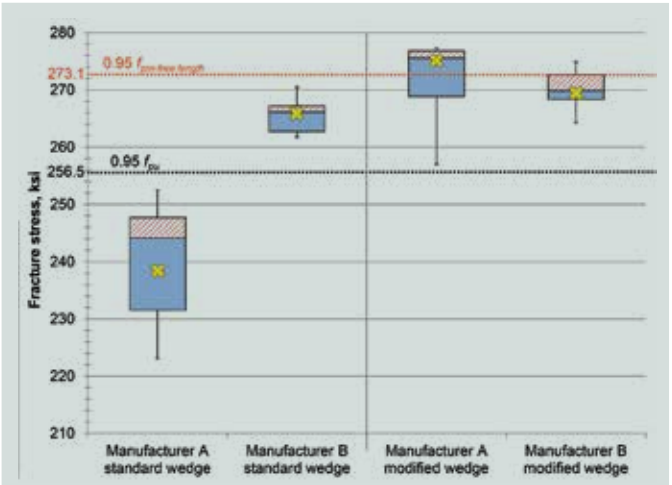

Figure 10. Box-and-whisker plots comparing manufacturer A and manufacturer B with standard and modified wedge geometries. Note: $f_{pm,free\text{-}length}$ = free-length fracture stress calculated by dividing the breaking strength provided from a free-length fracture test by the nominal cross-sectional area of the strand; f_{pu} = specified ultimate tensile strength of prestressing strand. Note: 1 ksi = 6.895 MPa.

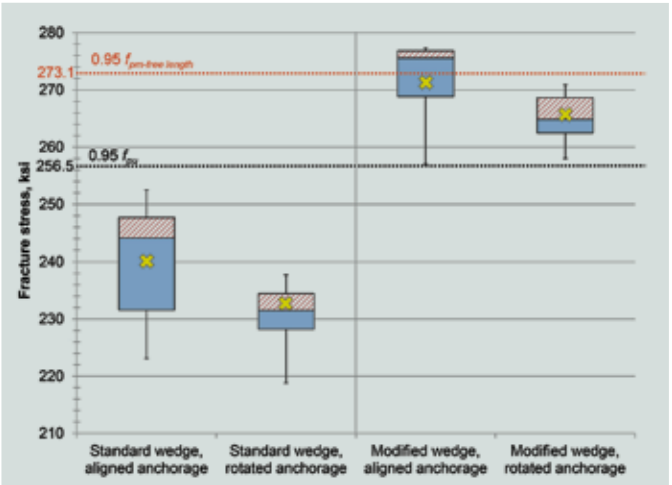

Figure 11. Box-and-whisker plots comparing aligned and rotated anchorages with standard and modified wedge geometries. Note: $f_{pm,free\text{-}length}$ = free-length fracture stress calculated by dividing the breaking strength provided from a free-length fracture test by the nominal cross-sectional area of the strand; f_{pu} = specified ultimate tensile strength of prestressing strand. Note: 1 ksi = 6.895 MPa.

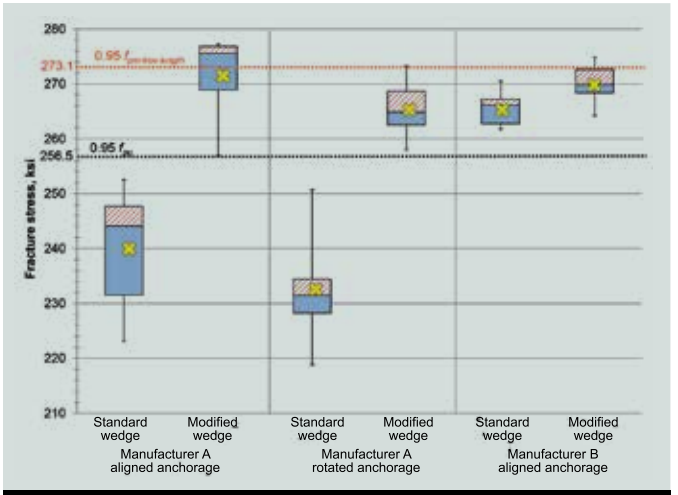

Figure 12. Box-and-whisker plots comparing standard and modified wedge geometries. Note: $f_{pm,free\text{-}length}$ = free-length fracture stress calculated by dividing the breaking strength provided from a free-length fracture test by the nominal cross-sectional area of the strand; f_{pu} = specified ultimate tensile strength of prestressing strand. Note: 1 ksi = 6.895 MPa.

tem was reduced when the anchorage ends were rotated, the reduction was not significant at a 95% confidence level.

A side-by-side comparison was made between the standard and modified wedge geometries for all of the tested configurations. The loading scheme parameter was previously eliminated, leaving three variables to be compared: wedge geometry, anchorage manufacturer, and anchorage alignment. **Figure 12** shows the box-and-whisker plot for the anchorages tested with standard and modified wedge geometries using the following:

- aligned anchors produced by manufacturer A
- rotated anchors produced by manufacturer A
- aligned anchors produced by manufacturer B

The calculated *p*-values for the manufacturer A–aligned, manufacturer A–rotated, and manufacturer B–aligned configurations are 3.249×10^{-4}, 4.945×10^{-5}, and 0.0604, respectively. This indicates that the modified wedge geometry significantly increased the fracture strength for anchorages from manufacturer A when tested in both the aligned and rotated configurations. The modified wedge also increased the mean fracture strength capacity of anchorages from manufacturer B; however, the increase was not significant using a 95% confidence interval.

Strain capacity

The strain capacity of the multistrand posttensioning anchorage system was analyzed in terms of microstrain as determined by strain gauges applied to an individual wire of each strand (that is, one strain gauge per strand). **Figures 13** and **14** present the maximum fracture and ultimate strain values. The maximum strain is defined as the maximum strain reading of all working strain gauges at a particular time. While this value is less conservative than the average strain, the researchers believe it is a more accurate representation of the limiting strand strain that would be observed in a full-scale application due to the longer strand lengths resulting in a more uniform strain distribution.

Figure 13 shows the results for the monotonically loaded tests, and Fig. 14 shows the results from the cyclically loaded tests. Three repetitions were conducted for each configuration, represented by vertical bars. The lower (solid) part of the bar represents the fracture strain of the system, and the upper (crosshatched) part of the bar represents the ultimate strain of the system. If the bar is completely solid, the ultimate strain is equal to the fracture strain. The deformation requirement of 2.0% at ultimate is also indicated on each graph.

As shown in Fig. 13 and 14, on average the anchorages from both manufacturers tested with standard wedges did not meet the elongation requirement of 2.0% at ultimate. The fact that the standard wedges from manufacturer B did meet the $0.95f_{pu}$ strength limit at fracture (Fig. 8 and 9) indicates another discrepancy in the ACI 318-14 certification requirements. That is, the system was able to meet the strength requirement without meeting the elongation requirement. This is essentially due to the fact that $0.95f_{pu}$ (256.5 ksi [1769 MPa]) does not correspond to a strain of 2.0% on the PCI-defined stress-strain curve for posttensioning strand. Rather, a strand strain of 2.0% corresponds to a stress of about 264.3 ksi (1822 MPa), or $0.98f_{pu}$. Essentially, this makes the less stringent strength limit of $0.95f_{pu}$ inconsequential because the strain limit will always control. However, in the case of the more stringent

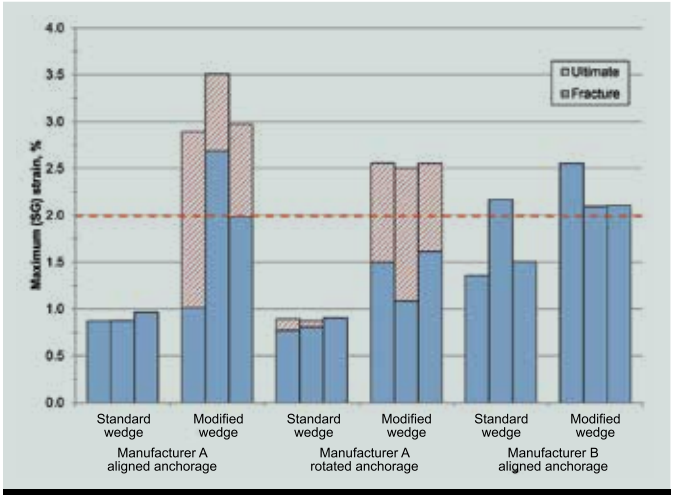

Figure 13. Summary of maximum strain results for monotonically loaded specimens.

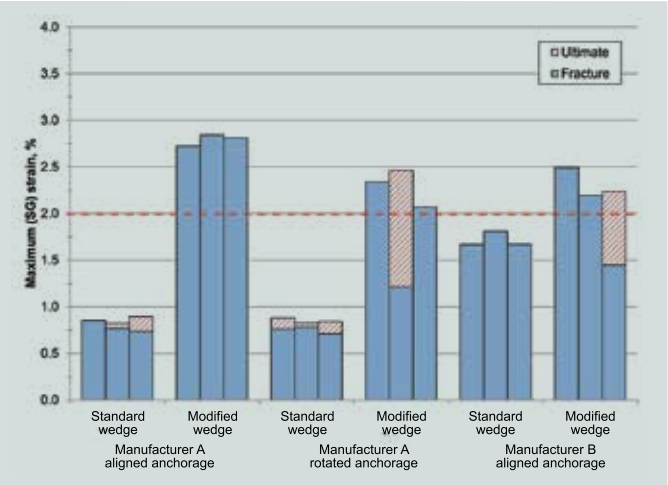

Figure 14. Summary of maximum strain results for cyclically loaded specimens.

$0.95f_{pm,free\text{-}length\ limit}$, the strength requirement may or may not control, depending on the actual breaking strength of the strand. For this reason, it is recommended that the strength limit of $0.95f_{pm,free\text{-}length}$ be adopted by ACI 318.

In each of the configurations using the modified wedge geometry, the elongation requirement of 2.0% at ultimate is always achieved. However, the preferred limiting strain in terms of the design of rocking structures is the fracture strain. While the modified wedge geometry allowed fracture strains of more than 2.5% in some cases, premature fractures were also recorded at strains as low as 1.0% when the modified wedge was being used. This large range in maximum fracture strain indicates the need for further research in the area of improved wedge geometry. In addition, the possibility of wire fractures at strains as low as 1.0% requires that a strand strain limit of 1.0% elongation be used at a desired drift in the design of self-centering structures with unbonded posttensioning. Wedges with the modified geometry were used in a parallel shake table test investigation of rocking walls.[23] All posttensioning tendons in these walls were designed to remain elastic at the design drift. Although these tendons experienced strains as high as 1.5%, there was no evidence that wire fracture occurred.

Conclusion

This paper presents results from a comprehensive laboratory evaluation of the fracture and ultimate strengths and strain capacities of multistrand posttensioning anchorage systems. Recognizing that the strength and strain capacities for strands provided in mill certificates are established using special wedges, the tests in this study were conducted using commercially available wedges to establish realistic stress and strain limits for the use of unbonded tendons in the seismic design of rocking structures. Due to the increased variability in strain distributions amongst strands after yielding, a posttensioning tendon consisting of several strands often experiences fracture of an individual wire at a load less than the ultimate strength. For this reason, the strength and deformation capacities of the system were analyzed in terms of both fracture and ultimate strength and strain. According to the terminology used in ICC-ES AC303 for determination of certification compliance, the fracture strength of the system is compared with the strength limits, and the ultimate strain is compared with the deformation limit.

Based on the completed study, the following results regarding certification conformance of multistrand posttensioning anchorages were observed:

- The multistrand anchorage system only met both the strength ($0.95f_{pu}$) and deformation (2.0%) requirements of ACI 318-14 when the modified wedge geometry was used.
- Only one of the tested configurations (aligned anchorages from manufacturer A with modified wedges loaded cyclically) met both the strength ($0.95f_{pm,free\text{-}length}$) and deformation (2.0%) requirements of ICC-ES AC303.
- Anchorages from manufacturer A with standard wedges were the only configurations that failed to meet the ACI 318-14 strength requirement of $0.95f_{pu}$.
- Anchorages from manufacturer B with standard wedges met the ACI 318-14 strength requirement ($0.95f_{pu}$), but not the deformation requirement of 2.0% strain limit.

Regarding the test variables and configurations investigated, the following conclusions can be made:

- The cyclic loading scheme implemented in this paper did not significantly affect the performance of the system under any configuration.
- The performance of the systems varied greatly depending on the anchorage manufacturer; however, neither anchorage was found to be superior. Rather, it was determined that compatibility of the anchorages and wedges is the primary factor in anchorage performance.
- Rotation of an anchorage inducing the effects of eccentricity, an angled entrance of the strand into the anchorage, and fretting did not significantly affect the performance of the prestressing tendon.
- The geometrically modified wedge significantly improved the performance of anchorages produced by manufacturer A. They also allowed anchorages from manufacturer B to meet the strength and deformation requirements of ACI 318-14, though the improvement was not statistically significant at a 95% confidence interval.

Furthermore, based on the investigation presented in this paper, the following recommendations are made:

- Unbonded posttensioned rocking structures should be detailed by the structural design engineer to include wedges following the modification principles presented in this study.
- If individual wire fracture is considered unacceptable, a strand strain limit of 1.0% should be used in the design of unbonded posttensioning in rocking structures, even when designed with the modified wedge geometry. When individual wire fractures are acceptable, this strain limit may be increased to 2% for the modified wedge geometry.
- The more stringent strength requirement of $0.95f_{pm,free\text{-}length}$ should be adopted by ACI 318 because the current limit ($0.95f_{pu}$) does not correlate to the deformation requirement (2.0% strain) based on the PCI-defined stress-strain relationship of posttensioning strand.
- Further research should be conducted on the relationship between individual wire strain determined using strain gauges and strand elongation as a whole.
- Further research should be conducted in the area of wedge geometry development, especially regarding the modified wedge geometry principles.

For the purpose of developing acceptance testing criteria for multistrand posttensioning anchorages in which multiple strands are loaded simultaneously, it is recommended that:

- each strand be instrumented such that the strain in each strand is recorded
- wedges at each end of the assembly be hand- or power-seated to a constant load (less than 1000 lb [4450 N]) prior to the application of the preload
- specimens with an absolute strain differential between strands greater than a strain of 0.2% at any point in the loading up to $0.80f_{pu}$ should be discarded and the test repeated
- limits relevant to current multistrand posttensioning anchorage systems be developed based on achievable fracture and ultimate strength and strain capacities
- fracture stress and strain values be compared with the more stringent strength ($0.95f_{pm,free\text{-}length}$) and elongation (2.0%) limits introduced by PTI, based on the current limits in place

Acknowledgments

The authors would like to thank the National Science Foundation for providing the financial support to complete the research summarized in this paper through CMMI grant 1041650. All opinions, findings, and conclusions or recommendations expressed in this paper are those of the authors and do not necessarily reflect the views of the National Science Foundation. The modified wedges were manufactured and supplied by Precision-Hayes, formerly Hayes Industries Ltd., and the strands were donated by Sumiden Wire Products Corp. (SWPC). The authors thank Randy Draginis of Precision-Hayes and Jeff Feitler of SWPC for their support and advice during the course of the experimental study.

References

1. ACI (American Concrete Institute) Committee 423. 2014. *Specification for Unbonded Single-Strand Tendon Materials*. ACI 423.7-14. Farmington Hills, MI: ACI.
2. ACI Committee 423. 2005. *Recommendations for Concrete Members Prestressed with Unbonded Tendons*. ACI 423.3-05. Farmington Hills, MI: ACI.
3. PTI (Post-Tensioning Institute). 2000. *Specification for Unbonded Single Strand Tendons*. PTI M10.2-00. Phoenix, AZ: PTI.
4. ACI Committee 318. 2014. *Building Code Requirements for Structural Concrete (ACI 318-14) and Commentary (ACI 318R-14)*. Farmington Hills, MI: ACI.
5. Walsh, K. Q., and Y. C. Kurama. 2010. "Behavior of Unbonded Post-tensioning Monostrand Anchorage Systems under Monotonic Tensile Loading." *PCI Journal* 55 (1): 97–117.
6. Walsh, K. Q., and Y. C. Kurama. 2012. "Effects of Loading Conditions on the Behavior of Unbonded Post-tensioning Strand-Anchorage Systems." *PCI Journal* 57 (1): 76–96.
7. Walsh, K. Q., R. L. Draginis, R. M. Estes, and Y. C. Kurama. 2013. "Effects of Anchor Wedge Dimensional Parameters on Post-Tensioning Strand Performance." Structural Engineering Research Report NDSE-2013-02. Department of Civil and Environmental Engineering and Earth Sciences, University of Notre Dame.
8. Musselman, E. S., M. Fournier, P. McAlpine, and S. Sritharan. 2015. "Behavior of Unbonded Post tensioning Monostrand Anchorage Systems under Short Duration, High Amplitude Cyclical Loading." *Engineering Structures* 104: 116–125.

9. PTI (Post-Tensioning Institute). 1998. *Acceptance Standards for Post-tensioning Systems*. PTI M50.1-98. Farmington Hills, MI: PTI.

10. Hayes, N. O., and R. Draginis. 2010. Anchor wedge configuration for tendon anchors. US Patent 7,726,082 B2, filed December 4, 2004, and issued June 1, 2010.

11. Corven, J., and A. Moreton. 2013. "Appendix A–Terminology." In *Post-Tensioning Tendon Installation and Grouting Manual*. Version 2.0. FHWA-NHI-13-026. Washington, DC: U.S. Department of Transportation, Federal Highway Administration.

12. Nakaki, S. D., J. F. Stanton, and S. Sritharan. 1999. "An Overview of the PRESSS Five-Story Precast Test Building." *PCI Journal* 44 (2): 26–39.

13. Priestley, M. J. N., S. Sritharan, J. R. Conley, and S. Pampanin. 1999. "Preliminary Results and Conclusions from the PRESSS Five-Story Precast Concrete Test Building." *PCI Journal* 44 (6): 42–67.

14. Sritharan, S. 2002. "Performance of Four Jointed Precast Frame Systems under Simulated Seismic Loading." In *Proceedings of the Seventh National Conference on Earthquake Engineering, July 21-25, 2002, Boston, Mass*. Oakland, CA: Earthquake Engineering Research Institute.

15. Sritharan, S., S. Aaleti, R. S. Henry, K.-Y. Liu, and K.-C. Tsai. 2015. "Precast Concrete Wall with End Columns (PreWEC) for Earthquake Resistant Design." *Earthquake Engineering and Structural Dynamics* 44 (12): 2075–2092. doi: 10.1002/eqe.2576.

16. ACI Innovation Task Group 5. 2008. *Acceptance Criteria for Special Unbonded Post-tensioned Precast Structural Walls Based on Validation Testing.* ACI ITG-5.1-07. Farmington Hills, MI: ACI.

17. ASTM Subcommittee A01.05. 2016. *Standard Specification for Low-Relaxation, Seven-Wire Steel Strand for Prestressed Concrete*. ASTM A416/A416M-16. West Conshohocken, PA: ASTM International.

18. ASTM Subcommittee A04.02. 2014. *Standard Specification for Ductile Iron Castings*. ASTM A536-84. West Conshohocken, PA: ASTM International.

19. Hayes, N. O., and R. Draginis. 2010. Anchor system with substantially longitudinally equal wedge compression. US Patent 7,765,752 B2, filed February 20, 2008, and issued August 3, 2010.

20. International Code Council Evaluation Service (ICC-ES). 2007. *Acceptance Criteria for Post-Tensioned Anchorages and Couplers of Prestressed Concrete.* Evaluation Report AC303. Whittier, CA: ICC-ES.

21. Yates, D. L. 1988. "A Study of Fretting Fatigue in Post-Tensioned Concrete Beams." MS thesis. University of Texas at Austin.

22. Acosta, J. A. A. 1991. "Instrumentation Systems for Post-Tensioned Segmental Box Girder Bridges." MS thesis. University of Texas at Austin.

23. Nazari, M., S. Sritharan, and S. Aaleti. 2014. "An Experimental Evaluation of Unbonded Post-tensioned Precast Rocking Walls." In *Proceedings of the 60th PCI Convention and National Bridge Conference, September 6–9, 2014, National Harbor, Md.* Chicago, IL: PCI. CD-ROM.

Notation

BID = inside diameter of anchor bottom

BW = outside width of wedge bottom

d_a = outside crown-to-crown diameter of prestressing strand

D_{mw} = diameter of middle prestressing strand wire

D_{ow} = diameter of outer prestressing strand wire

H = height of component

$f_{pm,free\text{-}length}$ = free-length fracture stress calculated by dividing the breaking strength provided from a free-length fracture test by the nominal cross-sectional area of the strand

f_{pu} = specified ultimate tensile strength of prestressing strand

IW = inside width of wedge

p-value = result of a t-test that indicates the probability of the null hypothesis being correct

P = pitch of prestressing strand

RAD = distance from centerline of anchor to centerline of wedge opening

TID = inside diameter of anchor top

TW = outside width of wedge top

About the authors

Daniel Abramson, PE, is an engineer with Permasteelisa North America in Minneapolis, Minn. Permasteelisa is a contractor in the engineering, project management, manufacturing, and installation of architectural envelopes and interior systems. He earned his BS in civil engineering from the University of Minnesota Duluth in 2012 and his MS in 2013. His MS research focused on the performance of multistrand posttensioning anchorage systems for use in seismic-resilient rocking wall structures.

Eric Musselman, PhD, PE, is an assistant professor in the department of Civil and Environmental Engineering at Villanova University in Villanova, Pa. He is a member of the American Concrete Institute, where he chairs Committee 435, Deflections of Concrete Structures, and also of the Post-Tensioning Institute. He is actively involved in research related to the performance and durability of posttensioned systems. He earned his PhD from Pennsylvania State University in 2007.

Sri Sritharan, PhD, FACI, is the Wilkinson Chair and Interim Assistant Dean in the College of Engineering and Professor of Structural Engineering in the Department of Civil, Construction and Environmental Engineering at Iowa State University in Ames, Iowa. He has been actively involved with PCI and PCI committees in the area of precast/prestressed concrete structural systems for seismic applications. He served as the project manager during phase 3 of the PRESSS program at the University of California, San Diego, where he also earned his PhD in structural engineering.

Abstract

The growing popularity of unbonded posttensioned structures designed for seismic resiliency, in conjunction with recent research indicating the inability of commercially available posttensioning anchorage systems to meet current industry certification standards, has prompted the need to investigate and better understand posttensioning anchorage systems. Recent research has focused on single-strand posttensioning systems; however, virtually no published literature is available regarding the behavior of multistrand anchorages. This paper presents results from a comprehensive laboratory evaluation of the fracture and ultimate strength and strain capacities of multistrand posttensioning anchorage systems for use in seismic-resilient rocking structures. The testing program encompassed two anchorage manufacturers, two anchorage alignment configurations, and two wedge geometries under both monotonic and cyclic loading. The results show that modifying the wedge geometry can improve the performance of commercially available posttensioning anchorages and that a strain limit of 1% should be used for seismic applications.

Keywords

Anchorage, multistrand, posttensioning, posttensioning anchorages, rocking, seismic, strain capacity, wall, wedge.

Review policy

This paper was reviewed in accordance with the Precast/Prestressed Concrete Institute's peer-review process.

Reader comments

Please address reader comments to journal@pci.org or Precast/Prestressed Concrete Institute, c/o *PCI Journal*, 200 W. Adams St., Suite 2100, Chicago, IL 60606.